Astron. Astrophys. 353, L33–L36 (2000)

ASTRONOMY AND ASTROPHYSICS

LETTER

*Letter to the Editor*

# An extrasolar giant planet in an Earth-like orbit⋆

## Precise radial velocities of the young star $\iota$ Horologii = HR 810

**M. Kürster[1], M. Endl[1,2], S. Els[1,3], A.P. Hatzes[4], W.D. Cochran[4], S. Döbereiner[5], and K. Dennerl[5]**

[1] European Southern Observatory, Casilla 19001, Vitacura, Santiago 19, Chile
[2] Universität Wien, Institut für Astronomie, Türkenschanzstrasse 17, 1180 Wien, Austria
[3] Universität Heidelberg, Institut für Theoretische Astrophysik, Tiergartenstrasse 15, 69121 Heidelberg, Germany
[4] The University of Texas at Austin, McDonald Observatory, Austin, TX 78712-1083, USA
[5] Max–Planck–Institut für Extraterrestrische Physik, Giessenbachstrasse, 85748 Garching, Germany

Received 19 October 1999 / Accepted 7 December 1999

**Abstract.** We present 5 1/2 years of radial velocity (RV) monitoring with the ESO CES of the young (ZAMS) G0V star $\iota$ Hor. We find a Keplerian signal with a period of $320.1$ d indicative of an orbiting planet with minimum mass $m \sin i = 2.26\,\mathrm{M_{Jup}}$. With an eccentricity of $0.161$ and a semi-major axis of $0.925$ AU this object moves in the most Earth-like orbit found so far among extrasolar planets. $\iota$ Hor is the youngest star with a known planet. In addition to the planetary signal we find an excess RV scatter of $27.0\ \mathrm{ms^{-1}}$ rms exceeding our measurement precision of $17.4\ \mathrm{ms^{-1}}$ and probably due to stellar activity.

**Key words:** stars: planetary systems – stars: individual: $\iota$ Hor – stars: rotation – techniques: radial velocities

### 1. Introduction

Differential radial velocity (RV) measurement of the reflex motions of late-type stars is currently the most successful method for the discovery of extrasolar giant planets (e.g.: Latham et al. 1989; Mayor & Queloz 1995; Marcy & Butler 1996; Noyes et al. 1997; Cochran et al. 1997) and of planetary systems (Butler et al. 1999).

Several of the properties of the new planets were unexpected such as orbital periods of a few days and orbital eccentricities exceeding those of the solar system giant planets. This has implications for the question when and where planets form in the protoplanetary disk.

It is therefore important to search for planets around stars as young as possible. However, the activity of young stars can deteriorate the precision at which stellar RVs can be measured as stellar rotation changes the visibility of active regions (star spots, granulation patterns) and introduces variations of the stellar absorption line shapes which, if unresolved, lead to erroneous RV values (Saar & Donahue 1997; Saar et al. 1998). Therefore, all ongoing RV surveys (except the Keck Hyades search by Hatzes & Cochran, 1999) have deliberately excluded active stars.

In this paper we present RV data of $\iota$ Hor whose activity produces an excess data scatter exceeding the measurement error. Nevertheless, a sufficient time baseline and a large number of measurements enable us to detect the signal of an orbiting giant planet. We have earlier identified $\iota$ Hor as the most variable star in our sample (Hatzes et al. 1996) and, after 4 yr of observations with sparse sampling, found (with low confidence) what appeared to be an eccentric Keplerian signal with a $600$ d period (Kürster et al. 1998, 1999a). Another 1.5 yr of intensified monitoring permits us now to uncover a near-sinusoidal signal with a $320$ d period as the true source of this variation.

### 2. The planet search program and data modelling

In Nov. 1992 we began a program for the search for extrasolar planets at ESO La Silla using the 1.4m CAT telescope and the CES spectrograph equipped with the Long Camera and CCDs $\#30$ or $\#34$ yielding a resolving power of $R = 100,000$, a central wavelength of $5389$ Å, and a spectrum length of $48.5$ Å. We self-calibrated the CES with a temperature controlled (at $50^\circ$ C) iodine ($I_2$) gas absorption cell that superimposes its absorption lines onto the stellar spectrum (Kürster et al. 1994; Hatzes et al. 1996; Hatzes & Kürster 1994). This technique provides high measurement precision for differential RVs.

The data analysis presented in this paper (Sect. 4) makes use of a recent improvement of our data modelling technique which we will describe in more detail in a forthcoming paper (Endl et al., in prep.; see also Endl et al. 2000). We largely follow the approach by Butler et al. (1996) and Valenti et al. (1995) synthesizing the observed star+iodine spectrum by higher resolution versions of pure iodine and pure star spectra and employing multi-parameter optimization and modelling of the instrumental

*Send offprint requests to*: M. Kürster (mkurster@eso.org)

⋆ Based on observations collected at the European Southern Observatory, La Silla

**Table 1.** The differential RV measurements of $\iota$ Hor

| BJD | $\Delta$RV[$\mathrm{ms}^{-1}$] | BJD | $\Delta$RV[$\mathrm{ms}^{-1}$] |
|---|---|---|---|
| 2,448,930.747 | −10.2± 9.2 | 2,450,524.542 | −45.2±12.5 |
| 2,448,973.742 | 9.5±14.1 | 2,450,524.552 | −26.8±17.5 |
| 2,449,055.524 | 59.9±14.0 | 2,450,551.481 | −2.8±12.4 |
| 2,449,245.916 | 78.0±26.8 | 2,450,647.923 | 32.4±34.1 |
| 2,449,310.713 | 36.8±17.8 | 2,450,647.934 | 19.0±27.5 |
| 2,449,357.652 | 46.0±21.0 | 2,450,689.910 | −33.5± 5.2 |
| 2,449,357.673 | 49.8±15.5 | 2,450,689.923 | −14.1±22.6 |
| 2,449,412.532 | 37.4±19.9 | 2,450,703.914 | −27.6±21.9 |
| 2,449,549.862 | −36.0±13.5 | 2,450,703.926 | −39.1±14.6 |
| 2,449,601.889 | 29.5±36.9 | 2,450,704.808 | −10.5±25.3 |
| 2,449,684.638 | 87.3±11.9 | 2,450,704.820 | −56.4±10.8 |
| 2,449,684.660 | 77.5±15.0 | 2,450,709.798 | −3.6±20.1 |
| 2,449,730.649 | 63.9±19.7 | 2,450,709.803 | 2.1±16.0 |
| 2,449,730.671 | 83.9±27.0 | 2,450,709.818 | −31.3±32.5 |
| 2,449,907.884 | −16.0±10.1 | 2,450,720.882 | −20.3±18.6 |
| 2,450,016.743 | 59.3±16.7 | 2,450,720.893 | −59.7±19.2 |
| 2,450,085.704 | −33.7±20.1 | 2,450,720.905 | −11.2±22.9 |
| 2,450,086.703 | −38.7±24.0 | 2,450,722.824 | −57.8± 7.6 |
| 2,450,145.558 | −21.5±26.3 | 2,450,722.835 | −53.2±22.0 |
| 2,450,301.919 | 99.0±23.1 | 2,450,722.847 | −76.4± 9.0 |
| 2,450,304.800 | 60.0±21.1 | 2,450,733.840 | −33.9±16.9 |
| 2,450,313.872 | 67.0± 8.2 | 2,450,733.851 | −22.8±20.2 |
| 2,450,314.927 | 62.2±13.7 | 2,450,733.863 | −43.0±15.7 |
| 2,450,323.747 | 79.0± 3.9 | 2,450,751.779 | −50.0± 9.3 |
| 2,450,325.740 | 46.8±22.8 | 2,450,751.791 | −26.9±18.9 |
| 2,450,330.883 | 64.8±12.9 | 2,450,751.802 | −55.7±28.2 |
| 2,450,348.694 | 104.3±33.6 | 2,450,752.711 | −52.6± 8.0 |
| 2,450,348.706 | 118.3±17.7 | 2,450,752.722 | −75.4±17.3 |
| 2,450,348.717 | 106.0±25.2 | 2,450,753.650 | −82.4±25.6 |
| 2,450,349.848 | 120.7±13.9 | 2,450,753.662 | −72.9±12.7 |
| 2,450,357.814 | 37.8±20.2 | 2,450,753.673 | −63.5±17.5 |
| 2,450,358.768 | 59.8±19.4 | 2,450,818.667 | −44.4±29.9 |
| 2,450,359.806 | 24.3±12.6 | 2,450,819.639 | −53.0±10.5 |
| 2,450,385.722 | 28.9± 9.3 | 2,450,819.651 | −59.8±12.9 |
| 2,450,386.634 | −2.2±25.2 | 2,450,820.704 | −57.9±20.0 |
| 2,450,386.646 | 18.3± 9.7 | 2,450,820.716 | −72.5±18.1 |
| 2,450,386.658 | −11.2±25.7 | 2,450,854.636 | −30.6±14.4 |
| 2,450,386.669 | 7.8±17.9 | 2,450,855.598 | −48.0±21.1 |
| 2,450,417.793 | −47.4±15.8 | 2,450,855.610 | −25.5± 8.8 |
| 2,450,417.805 | −44.7±20.7 | 2,450,856.612 | −23.5±12.9 |
| 2,450,417.817 | −11.7±13.5 | 2,450,856.623 | 1.6± 6.2 |
| 2,450,418.739 | −17.7± 5.2 | 2,450,897.498 | 34.3±11.8 |
| 2,450,477.644 | −52.6±10.6 | 2,450,897.510 | 24.9± 5.6 |
| 2,450,477.656 | −60.8±18.1 | 2,450,898.511 | 15.5±14.5 |
| 2,450,478.649 | −42.0±10.3 | 2,450,898.522 | 40.6±25.2 |
| 2,450,478.660 | −61.5±16.0 | 2,450,907.475 | 61.8±17.1 |
| 2,450,523.518 | −22.2±16.6 | 2,450,907.487 | 73.2±18.9 |
| 2,450,523.530 | −39.5±20.7 | | |

profile (IP). Extending this approach we include model parameters specifically suited for the CES and various functions plus maximum entropy (MEM) reconstruction to treat the IP. As the IP varies along the spectrum each data set is subdivided into 25 individually modelled chunks of 80 pixels each. The mean value and rms scatter from all chunks provide an RV measurement and error. A pure iodine model at $R = 400,000$ was obtained by scanning our cell with the Kitt Peak FTS; we get stellar models of the same resolution by MEM deconvolution of pure star CES spectra with IPs reconstructed from CES iodine spectra. RVs are determined from the combined star+iodine model; if available, various pure star spectra are employed (cf. Kürster et al. 1999b). The data are corrected to the solar system barycenter with the JPL ephemeris DE200.

As we have shown for a constant star ($\tau$ Ceti) and for stars with known planets (51 Peg, 70 Vir) we now achieve a measurement precision of $14\ \mathrm{ms}^{-1}$ (Endl et al. 2000).

## 3. Stellar properties of $\iota$ Horologii

$\iota$ Hor (HR 810, HD 17051, HIP 12653) is a G0V star with $V = 5.40$ and a Hipparcos parallax of $58.00 \pm 0.55$ mas. CaII emission was found by Dravins (1981) and X-ray emission by Hünsch et al. (1998) indicating an active star. From CaII data Saar & Osten (1997) and Saar et al. (1997) estimate a rotation period of 7.9 d and 8.6 d, respectively.

Rocha-Pinto & Maciel (1998) measure a CaII index of $\log R'_{\mathrm{HK}} = -4.65$ indicating an age of $1.556$ Gyr, but find a contrasting value of $6.890$ Gyr from isochrone matching. They determine a sub-solar iron abundance $[\mathrm{Fe/H}] = -0.12$ and an effective temperature of $T_{\mathrm{eff}} = 6038$ K.

A recent analysis of the properties of $\iota$ Hor was communicated to us by Porto de Mello & da Silva (priv. comm.) who used spectra obtained with the Coudé spectrograph of the 1.60m telescope at Observatorio do Pico dos Dias. The results are $T_{\mathrm{eff}} = 6125 \pm 30$ K, surface gravity $\log g = 4.43 \pm 0.06$ dex, microturbulent velocity $1.64 \pm 0.13\ \mathrm{kms}^{-1}$, and luminosity $L = 1.52 \pm 0.05\ \mathrm{L}_{\odot}$ implying a radius of $R = 1.097 \pm 0.019\ \mathrm{R}_{\odot}$. From the lithium and barium abundances, $\log N(\mathrm{Li}) = 2.45$ and $[\mathrm{Ba/Fe}] = +0.17$, an age between 30 Myr and 2 Gyr is inferred, i.e. a zero-age main sequence (ZAMS) stage. In contrast to the previous authors Porto de Mello & da Silva determine a higher than solar iron abundance of $[\mathrm{Fe/H}] = +0.11 \pm 0.04$.

## 4. RV data for $\iota$ Horologii and period search

Our RV data for $\iota$ Hor are based on 95 spectra taken between late 1992 and early 1998. Exposure times were $15 - 30$ min and S/N values $150 - 250$. Table 1 lists our differential RVs together with their errors and the barycentrically corrected Julian day. In the modelling process we (successively) used 5 available pure star spectra thus obtaining 5 distinct RV data sets (cf. Sect. 2) that we averaged (after matching the RV zero points) to obtain the final RV measurement. For each data point the rms scatter of the values from the 5 different models was taken as the error. The result has a total rms scatter of $52.5\ \mathrm{ms}^{-1}$ and a mean error of $17.4\ \mathrm{ms}^{-1}$, slightly higher than the $14\ \mathrm{ms}^{-1}$ we get for other stars (Sect. 2).

We searched our data set for a periodic RV signal in the range $2 - 2000$ d using the periodogram by Scargle (1982). False alarm probabilities (FAP) for the various power levels were determined via a bootstrap randomization scheme (Murdoch et al. 1993; Kürster et al. 1996). Fig. 1a shows the power

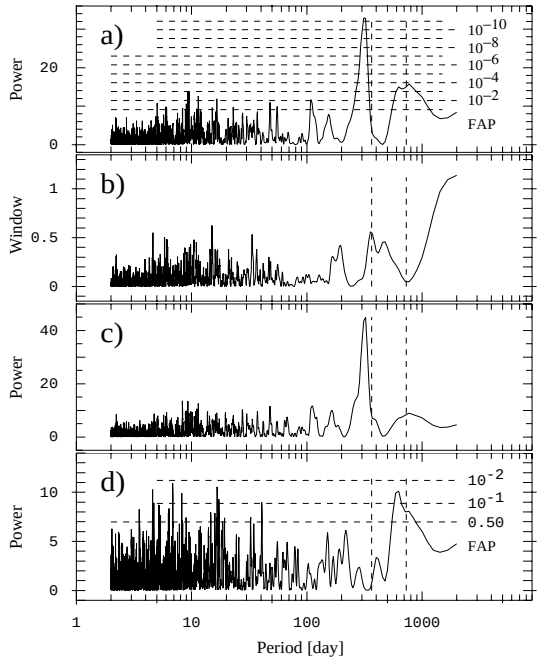


**Fig. 1a–d.** Periodogram for the RV data of $\iota$ Hor. Vertical dashed lines mark periods of 1 and 2 yr. Horizontal dashed lines in panels a and d give false alarm probabilities (FAP) **a**: Original data. **b**: Window function. **c**: RV data replaced by values from the best fit orbit. **d**: Residuals from the best fit orbit.

spectrum together with FAP levels. Periods of 1 and 2 yr are marked. The power spectrum is dominated by a peak at a period of 320 d with $FAP < 10^{-11}$ revealing a periodic signal. A second (blended) pair of peaks is found at periods 765 and 625 d with FAPs $< 10^{-3}$. Fig. 1b shows the window function that has a seasonal peak at 1 yr but is low at 320 d and 2 yr. To assess the amount of spectral leakage Fig. 1c shows the power spectrum for the data set where all RV data were replaced by the values from the best-fit orbital solution for the 320 d period (see Sect. 5). Some power is still found near 2 yr, hence the double peak in Fig. 1a is partly attributable to spectral leakage from the main signal. Fig. 1d shows the power spectrum for the residuals from the best-fit orbit. The double structure around 2 yr is still present now peaking at 600 d. The highest peak appears at 6.865 d, not far from the estimated rotation period (Sect. 3). However, adopting $FAP < 10^{-3}$ as the criterion for a significant signal we conclude that none of the peaks in the power spectrum of the residuals indicates the discovery of a second signal.

The question arises whether the 320 d period is significantly different from 1 yr, a periodicity that could stem, e.g., from a wrong barycentric correction. The value of 1 yr falls within the main periodogram peak, but in its wing, i.e. clearly resolved and with a strongly reduced power of 3.8 (high FAP) as opposed to 33.7 at maximum. Employing bootstrap randomization to determine the number of independent frequencies between $P = 320$ d and $P = 1$ yr (cf. Kürster et al. 1996) we find the two values separated by 1.8 independent frequency intervals. We can thus exclude that we see an artifact of a 1-yr periodicity.

**Table 2.** Parameters of the planet around $\iota$ Hor

| | |
|---|---|
| Orbital period | $P = 320.1 \pm 2.1$ d |
| Time of maximum RV | $T_\circ = \mathrm{BJD}2,450,307.0 \pm 3.0$ |
| RV semi-amplitude | $K = 67.0 \pm 5.1$ ms$^{-1}$ |
| Orbital eccentricity | $e = 0.161 \pm 0.069$ |
| Anomaly | $\omega = 83^\circ \pm 11^\circ$ |
| Minimum planet mass | $m \sin i = 2.26 \pm 0.18$ M$_{\rm Jup}$ |
| Orbital semi-major axis | $a = 0.925 \pm 0.104$ AU |

## 5. Orbital solution and companion parameters

The time baseline of our data set is 6.175 cycles of the 320 d signal indicating that it is stable and consisting of the reflex motion of $\iota$ Hor due to an orbiting companion. Fig. 2a shows the time series of the RV data together with the best-fit Keplerian orbit; Fig. 2b shows the residuals. In Fig. 3 the data are shown folded with the orbital period. The parameters of the orbital solution are listed in Table 2.

Adopting a stellar mass of $M = 1.03 \pm 0.02$ M$_\odot$ we find a minimum companion mass of $m \sin i = 2.26 \pm 0.18$ M$_{\rm Jup}$, where $i$ is the unknown orbital inclination. Assuming a companion orbit coplanar with the stellar equator we can determine $i$ by measuring the projected stellar rotation velocity $v \sin i$ and comparing it with the rotation velocity $v$ as calculated from the stellar radius $R$ and rotation period $P_{\rm rot}$. Kurucz model atmosphere fits to our pure star spectra yield $v \sin i = 5.5 \pm 0.5$ kms$^{-1}$ in agreement with Saar & Osten (1997) who find $5.7 \pm 0.5$ kms$^{-1}$. Using $R = 1.097 \pm 0.019$ R$_\odot$ and $P_{\rm rot} = 7.9 - 8.6$ d (Sect. 3) we get $v = 6.73 \pm 0.31$ kms$^{-1}$, hence $i = 47.2^\circ - 64.3^\circ$ (Saar & Osten 1997 give $37^\circ - 90^\circ$) and $m = 2.31 - 3.32$ M$_{\rm Jup}$. A drawback of this calculation is the poorly known value of $P_{\rm rot}$. However, mass upper limits can also be obtained from probability arguments for the orientation of the orbital plane (cf. Kürster et al. 1999b) that yield a confidence of 90% (95%, 99%) that the true mass $m < m \sin i \times 2.294\ (3.203,\ 7.088)$, i.e. $m < 5.18\ (7.24,\ 16.0)$ for the respective confidence level.

Thus the companion to $\iota$ Hor appears to be a massive Jupiter-like planet. With an orbital semi-major axis of $a = 0.925 \pm 0.104$ AU and eccentricity of $e = 0.161 \pm 0.069$ it has the most Earth-like orbit among the so far known extrasolar planets. Its periastron distance, $0.776 \pm 0.108$ AU, just exceeds Sun-Venus separation, its apastron distance, $1.075 \pm 0.136$ AU, is just above Sun-Earth separation. Its eccentricity is among the lower ones for extrasolar planets with periods of more than a month, but still greater than that of any solar system giant planet.

The rms scatter around the orbital solution, 27.0 ms$^{-1}$, is considerably higher than our measurement precision of 17.4 ms$^{-1}$. While we cannot exclude (nor confirm) the presence of additional periodic signals that could pertain to more planets (e.g. at periods longer than our time baseline, near 600 day, or at short periods; see Fig. 1d), much of this excess scatter is probably the result of stellar activity leading to variability with the rotation period as a result of visibility changes of active regions (cf. Sect. 1). But reconfigurations of active regions should prevent this signal to appear in the periodogram as its shape, phase,

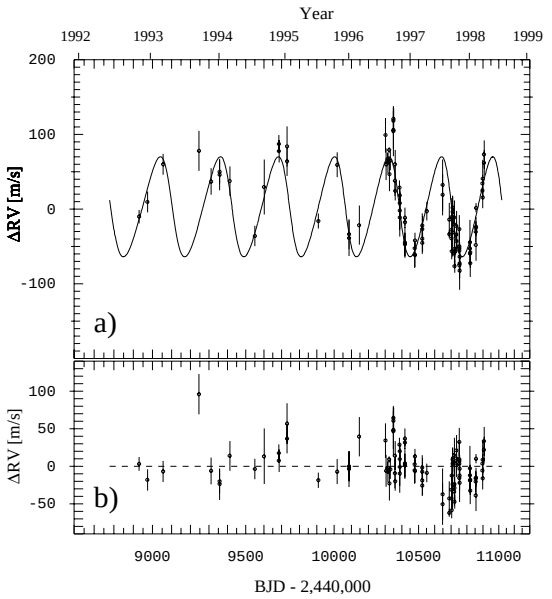


**Fig. 2a and b.** Time series of the differential RV data of $\iota$ Hor plotted vs. BJD (lower x-axis) and year (x-axis at top). **a**: RV data with overplotted best fit Keplerian orbit. **b**: Residuals.

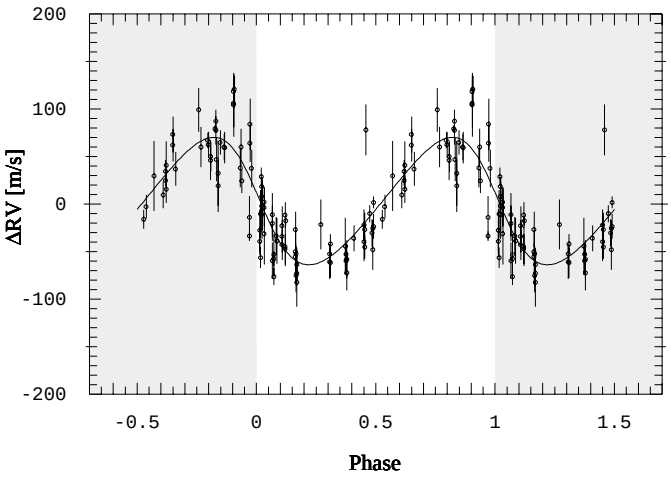


**Fig. 3.** The RV data of $\iota$ Hor plotted vs. orbital phase in the interval $[-0.5, 1.5]$. Each data point is plotted twice (repeated in the shaded area). The best fit Keplerian orbit is overplotted.

and amplitude change on short time scales. When the total scatter is corrected for the measurement precision (subtracted in quadrature) the remaining excess scatter is $20.6\ \mathrm{ms}^{-1}$, i.e. near the value of $16.1 \pm 3.5\ \mathrm{ms}^{-1}$ predicted by Saar et al. (1998) for a G-star with a rotation period of 8 day.

## 6. Conclusions

1. We have discovered an extrasolar giant planet in orbit around the G0V star $\iota$ Hor.
2. This planet has the most Earth-like orbit of all the so far discovered extrasolar planets.
3. Its eccentricity is greater than that of solar system giant planets just like that of the other known extrasolar planets with periods longer than a month.
4. This planet is the first one found around a young (ZAMS) star demonstrating the feasibility of applying the precision RV method to moderately active stars.

*Acknowledgements.* We thank the ESO OPC for generous allocation of observing time. The support of the 3.6m+CAT team, La Silla, and the Remote Control Operators, ESO Garching, was invaluable. We are indebted to G. Porto de Mello and L. da Silva for providing their results on $\iota$ Hor prior to publication. ME acknowledges support by the Austrian Fond zur Förderung der wissenschaftlichen Forschung Nr. S7302. APH and WDC acknowledge support by NASA grant NAG5-4384 and NSF grant AST-9808980. APH would like to thank I. Schutzmann for the inspiration behind this program.

## References

Butler R.P., et al.: 1999, ApJ, in press
Butler R.P., Marcy G.W., Williams E., McCarthy C., Dosanjh P., Vogt S.S.: 1996, PASP 108, 500
Cochran W.D., Hatzes A.P., Butler R.P., Marcy G.W.: 1997, ApJ 483, 457
Dravins D.: 1981, A&A 98, 367
Endl M., Kürster M., Els S.: 2000, in From Giant Planets to Cool Stars, ASP Conf. Ser., in press
Hatzes A.P., Cochran W.D.: 1999, Proc. VLT Opening Symposium 99, Springer Verlag, in press
Hatzes A.P., Kürster M.: 1994, A&A, 285, 454
Hatzes A.P., Kürster M., Cochran W.D., Dennerl K., Döbereiner S.: 1996, J. Geophys. Rev. (Planets), 101, 9285
Hünsch M., Schmitt J.H.M.M., Voges W.: 1998, A&AS 132, 155
Kürster M., Hatzes A.P., Cochran W.D., Pulliam C.E., Dennerl K., Döbereiner S.: 1994, The ESO Messenger, No. 76, 51
Kürster M., Hatzes A.P., Cochran W.D., Dennerl K., Döbereiner S., Endl M., Vannier M.: 1998, Workshop Science with Gemini, B. Barbuy, E. Lapasset, R. Baptista, R. Cid Fernandes (eds.), IAG-USP & UFSC 1998
Kürster M., Hatzes A.P., Cochran W.D., Dennerl K., Döbereiner S., Endl M.: 1999a, IAU Colloq. 170, J.B. Hearnshaw, C.D. Scarfe (eds.), PASP Conf. Ser. Vol. 185, 154
Kürster M., Hatzes A.P., Cochran W.D., Döbereiner S., Dennerl K., Endl M.: 1999b, A&A 344 L5
Kürster M., Schmitt J.H.M.M., Cutispoto G., Dennerl K.: 1996, A&A 320, 831
Latham D.W., Mazeh T., Stefanik R.P., Mayor M., Burki G: 1989, Nature 339, 38-40
Marcy G.W., Butler R.P.: 1996, ApJ 464, L147
Mayor M., Queloz D.: 1995, Nature 378, 355
Murdoch K.A., Hearnshaw J.B., Clark M.: 1993, ApJ 413, 349
Noyes R.W., et al.: 1997, ApJ, 483, L111
Rocha-Pinto H.J., Maciel W.J.: 1998, MNRAS 298,332
Saar S.H., Butler R.P., Marcy G.W.: 1998, ApJ 498, L153
Saar S.H., Donahue R.A.: 1997, ApJ 485, 319
Saar S.H., Huovelin R.A., Osten R.A., Shcherbakov A.G.: 1997, A&A 326, 741
Saar S.H., Osten R.A.: 1997, MNRAS 284, 803
Scargle J.D.: 1982, ApJ 263, 835
Valenti J.A., Butler R.P, Marcy G.W.: 1995, PASP 107, 966